Thin Solid Films 519 (2011) 2608–2612

Contents lists available at ScienceDirect

Thin Solid Films

journal homepage: www.elsevier.com/locate/tsf

Analysis of textured films and periodic grating structures with Mueller matrices: A new challenge in instrumentation with the generation of angle-resolved SE polarimeters

F. Ferrieu [c,*], T. Novikova [a], C. Fallet [a], S. Ben Hatit [a], C. Vannuffel [b], A. De Martino [a]

[a] LPICM, Ecole Polytechnique, F91128 Palaiseau, France
[b] CEA LETI MINATEC, F38054 Grenoble, France
[c] SERMA Technologies LETI MINATEC, F38054 Grenoble, France

ARTICLE INFO

Available online 21 December 2010

Keywords:
Polarimetry
Mueller matrix
Surface analysis
Scatterometry
Periodic structures
Gratings
Photonics structure
Angle-resolved polarimeter
Ellipsometer
Instrumentation

ABSTRACT

Current Mueller polarimeters, with either spectral or angular resolution, feature high enough precision and speed to be suitable for many demanding applications, with specific advantages over conventional spectroscopic ellipsometry (SE). Due to the simultaneous determination of depolarization, birefringence and diattenuation Mueller polarimetry (MP) can open new fields in surface and thin film characterization techniques with new and very powerful intrinsic analyses of roughness and/or anisotropy. For more conventional applications, such as scatterometry (i.e. the determination of the shape of periodic structures from optical measurements, mostly used in microelectronics), MP may overpass SE in terms of systematic errors and/or measurement spot size, as discussed from two examples. However, numerical simulations remain a key point to take full advantage of MP capabilities for the new challenges emerging in nanometrology.
© 2010 Published by Elsevier B.V.

1. Introduction

Polarimetry can be currently applied to nanotechnologies, surfaces, earth sciences, astrophysics, thin films interfaces and surface properties, photonics items, gratings, diffracting objects and living organisms in medicine. Although instrumental polarimetry began to be investigated 20 years ago, first with amplitude division polarimeters [1], this field is coming to maturity for applications only now, with considerable enhancements in precision and speed, as well as new features such as polarimetric imaging.

Non-periodic (rough) surfaces are generally characterized through the power spectral density (PSD) of their height distribution functions, determined from light scattering angular distributions. However, surface roughness may also induce light depolarization, a phenomenon which cannot be easily measured by usual spectroscopic ellipsometry (SE), nor modelled by the usual approach based on effective medium approximation. In fact, depolarization induced by surface roughness is becoming a challenging and very promising approach for surface characterization, especially with the repeatability and accuracy achieved by the current Mueller polarimeters. Reported Mueller matrices for surfaces with different roughnesses [2] corroborate the theoretical models.

Moreover, many applications of polarimetry exist in various fields such as scatterometry for lithography. Mueller polarimetry, with spectral and/or angular resolution, opens a new investigation domain for nanotechnologies, for materials as well as for gratings and photonic structures. Behind the instrumentation roadmap, numerical simulations of the polarimetric responses of the samples under study remain a key node for future commercial instruments.

In this contribution we first discuss the usefulness of full Mueller matrix measurements for rough (non-periodic) surfaces. Then the scope is broadened to periodic structure simulations. The light diffraction RCWA (rigorous coupled wave algorithm) theory and calculation algorithms have been widely described in the literature, but only few open source RCWA codes in the Mueller matrix formalism have been presented so far. This paper reports on some applications of this approach for surface analysis and scatterometry for lithography.

2. Theory

2.1. Characterisation of rough surfaces by depolarization

As it is well known, the Stokes–Mueller formalism can fully take into account the depolarization effects which may occur in any

* Corresponding author. Tel./fax: +334 76619365.
E-mail address: ferrieufr@gmail.com (F. Ferrieu).

0040-6090/$ – see front matter © 2010 Published by Elsevier B.V.
doi:10.1016/j.tsf.2010.12.062

polarimetric measurement, while this is not the case for the Jones formalism most widely used in classical ellipsometry.

Schematically, any Jones matrix [J] describing a given, non-depolarizing sample, may be associated to a non-depolarizing Mueller matrix [M_J]. Depolarization occurs whenever the Jones matrix [J] is no longer uniquely defined, due to sample in homogeneities, finite spectral or angular distribution of the incoming light, and the like. Then, the Mueller matrix [M] of the sample can be seen as a statistical (spatial, spectral, and/or temporal) average of the "elementary" [M_J] matrices. As a result, every Mueller matrix [M] is associated to a "coherency matrix" [T] [3,4] which is basically (via a suitable element permutation) the variance–covariance matrix of the statistical distributions of the elements of [M_J]. Like any variance–covariance matrix, [T] is hermitian, with four real, nonnegative eigenvalues λ_i.

If [M] is non-depolarizing (i.e. it is associated to a well-defined Jones matrix [J]), then one and only one λ_i is nonzero [3,4]. Depolarizing Mueller matrices can be characterized by their von Neumann entropy S, defined as

$$S = -\sum_{i=1}^{N} p_i \log_N p_i \tag{1}$$

where the p_i are given by

$$p_i = \frac{\lambda_i}{\sum_{j=1}^{N} \lambda_j} \tag{2}$$

S varies between 0, for nondepolarizing matrices, and 1 for "total" depolarizers, for which all the λ_i are equal [4].

An alternative quantifier of depolarization effects is the depolarization index P_d defined directly from the Mueller matrix elements M_{ij} as [5]:

$$P_d = \sqrt{\frac{\sum_{i,j=1}^{4} M_{ij}^2 - M_{11}^2}{3M_{11}^2}} \tag{3}$$

This index varies from 0, for "total" depolarizers, to 1, for non-depolarizing samples.

Most rough surfaces exhibit diagonal Mueller matrices (due to the absence of strong retardance and diattenuation effects). In this case, S and P_d are related by a "universal" relationship [6]:

$$S = -(3P_d + 1)/4\log_4\left(\frac{3P_d+1}{4}\right) - 3(1-P_d)/4\log_4\left(\frac{1-P_d}{4}\right) \tag{4}$$

2.2. Polarimetric characterization of surface by its angular distribution of slopes

We now assume that the surface roughness can be described by a uniform distribution of slopes with half width β_1 and a probability distribution $P(\beta) = \frac{1}{2\beta_1}$ for $\beta < \beta_1$ and zero otherwise. For each value of β the coherency matrix corresponding to the local specular reflection has to be rotated by this same angle β in a plane perpendicular to the scattering plane [3,4].Then the averaged <[T]> matrix becomes

$$\langle [T] \rangle = \int T(\beta) p(\beta) d\beta \tag{9}$$

In this case the polarimetric coherence γ, defined as

$$\gamma = \frac{\langle T_{12} \rangle}{\sqrt{\langle T_{11} \rangle \langle T_{22} \rangle}} \tag{10}$$

is less than 1. For the assumed model of distributions of slopes this coefficient turns out to be

$$\gamma = \frac{\mathrm{sinc}(2\beta_1)}{\sqrt{(1+\mathrm{sinc}(4\beta_1))}} \le 1 \tag{11}$$

where $\mathrm{sinc}(x) = \sin(x)/x$. Within this model the γ coefficient is related only to the roughness of the surface and not to its dielectric properties [4].

2.3. Experimental details and results

2.3.1. Polarimetric instrumentation

For the activities outlined in this contribution, we used two types of liquid crystal based Mueller polarimeters.

Spectrally resolved measurements were carried out with two commercially available instruments operating in the visible (450–850 nm), the MM-16 and the AutoSE, both from Horiba Scientific. These instruments were used to acquire complete Mueller spectra at discrete incidence and azimuthal angles, an approach which proved useful for the characterization of many samples, among which periodic structures representative of the current technology nodes [7].

An alternative implementation of Mueller polarimetry is with full angle resolution, by imaging the back focal plane of a high NA microscope objective [8]. The essential feature of this kind of instrument is to measure the Mueller matrix over all azimuths and incidences (limited by the objective NA) simultaneously, at discrete wavelengths. An updated scheme of the instrument available at LPICM is shown in Fig. 1.

Basically, this setup is a reflection microscope with a Köhler illumination scheme the source is imaged in the back focal plane (BFP) of the objective. In the output arm, a retractable lens allows to image either the sample itself, for real space Mueller microscopy, or the BFP, to measure the angular distribution of the emerging light (Fourier space Mueller imaging). In this latter case, due to the Abbe sine condition, in the image the radial coordinate is proportional to the sine of the incidence angle.

The polarization is modulated in the input arm by a liquid crystal based polarization state generator (PSG), and is analysed in the exit arm by a polarization state analyser (PSA), which is the 'mirror image" of the PSG. Two stops, respectively imaged on the BFP and on the

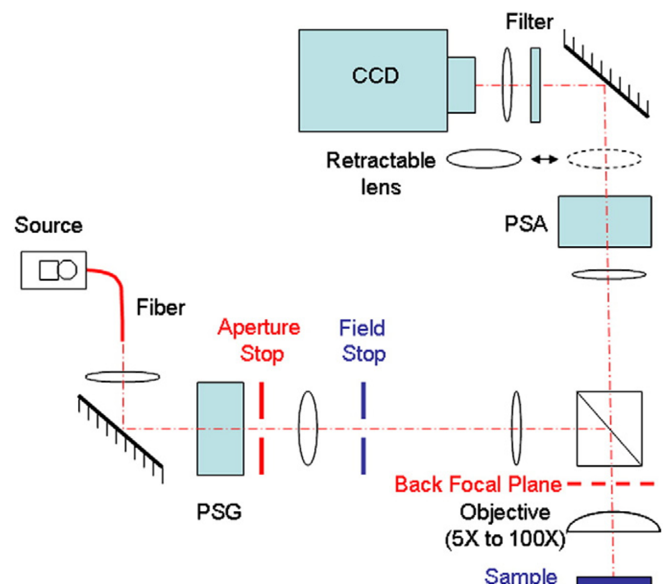

Fig. 1. Optical scheme of the angularly resolved Mueller polarimeter under development at LPICM. See text for details.

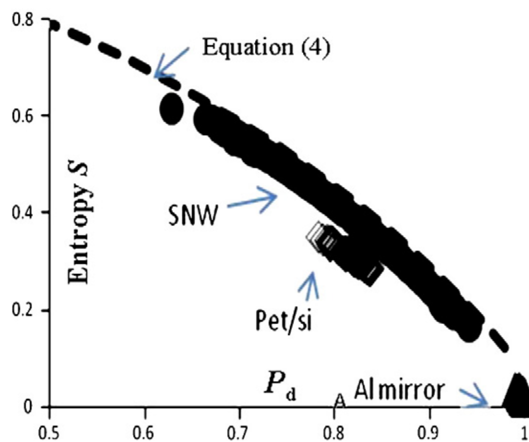

Fig. 2. Entropy versus depolarization P_d plot for several nanotechnology materials: with 70° incidence angle polarimetric spectroscopic measurements in the 1.5 and 3 eV range. The respective spectroscopic distributions (filled dots, squares, triangles) are compared with the plot of Eq. (4).

sample, allow to independently adjust the angular distribution of the light impinging on the sample (aperture stop) and the size of the illuminated area on the sample (field stop). As a result, this instrument allows polarimetric measurements on boxes as small as a few μm in lateral size, a feature which may constitute a great advantage over conventional low NA Spectroscopic Ellipsometry for metrology in microelectronics.

2.3.2. Light diffracted from rough surfaces

Several nanotechnology materials deposited in thin films were considered, namely smooth samples like aluminium (Al), low reflectivity thin films of plastic (PET), and silicon nanowires (SNW) deposited on silicon substrates. The [S, P_d] plot reconstructed from earlier published Mueller matrix data [1,9] as well as new measurements, is shown in Fig. 2.

In the relevant spectral range, the material optical indices remain quasi constant. Therefore the experimental points distributed along this curve are related to the micro crystals distribution density. Finally, the plastic PET film, with less micro impurities than Al samples, behave similarly, but the corresponding points are found well below the plot of Eq. (4), due to the PET optical anisotropy while Eq. (4) is valid only for optically isotropic materials.

On the other hand, the sensitivity of the parameter γ to the surface texture was verified by polarimetric measurements on both sides of a Silicon wafer (polished side with native oxide and rough backside of the wafer, with typical roughness of several μm, thus much larger than the wavelengths). The Mueller spectra were taken at 70° incidence and in the specular reflection direction for the emerging light. The result is shown in Fig. 3. The γ coherence factor decreases drastically for the wafer backside with respect to the polished side, and exhibits relatively weak variations with the photon energy, as expected from the model. We point out that SE measurements would not detect any depolarization effect, but would see only a shift in the Δ values and no changes in Ψ.

2.3.3. Periodic and photonic structures

Standard SE and, more recently, Mueller polarimetry have been applied to the characterization of periodic structures. The aim is to reconstruct the spatial profile of the structure from ellipsometric or polarimetric measurements, by solving the corresponding inverse diffraction problem. This scatterometry approach is currently used for nanolithography process control in microelectronics industry. Scatterometry is indeed fast and non-destructive, and provides much higher yields than other metrology techniques such as electron microscopy or AFM.

The usefulness of complete Mueller polarimetry at various azimuthal angles has been demonstrated with gratings etched in bulk silicon and accurately characterized by state of the art AFM-3D [7,10]. First, the measurement accuracy can be directly assessed by various redundancies present in full Mueller matrices and absent in standard SE. Second, the stability of the fitted model parameters when the azimuth is varied is a very valuable test the adequacy of the model chosen to describe the grating profiles.

Besides measurement aspects, the numerical simulations are crucial for a good overall performance. The rigorous coupled wave analysis, or RCWA, is now well established as a very general, yet numerically efficient, algorithm. Several RCWA codes are now available, among which the NIST Scatmech C++ library [11]. Several types of gratings can be considered in the RCWA class templates and

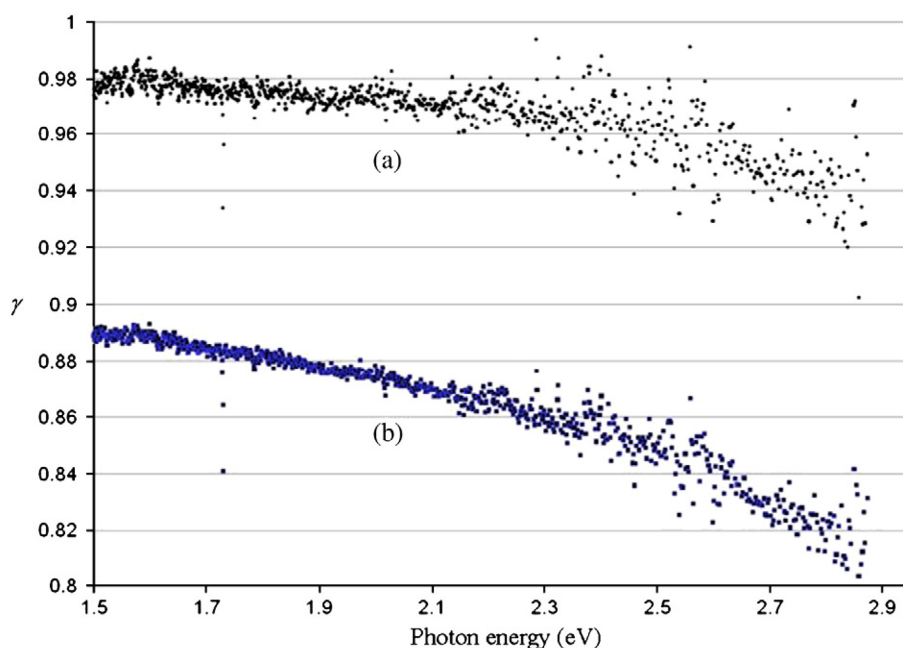

Fig. 3. 70° incidence γ factor measurements between 1.5 and 3 eV photon energies on both sides of a silicon wafer (polished side with native oxide and rough backside of the wafer.

the user can then modify the parameter values through usual pointer operations. To optimize the structure a rather complete analysis can be done through C++ non-linear optimization routine [12]. For more complicated structures a script file can be filled as, for example, in the case of a double patterning process[13].

But let us discuss again the value of the additional information provided by MP with respect to SE. The bottom panel of Fig. 4 shows a typical SE spectrum of the quantities usually called (α,β), corresponding in this case to $\alpha = -m_{12}$ and $\beta = m_{33}$ elements of the full Mueller matrix. These data were taken on a grating etched resist on top of bulk Si, and modelled by the symmetrical trapezoid with rounded corners shown in the top panel of the same figure. This model involves five parameters: the grating height (h), the top CD (w), the "footprint" of the sidewalls (a), and the top and bottom radii of curvature (R_t, R_b). This model clearly provides a good fit of the experimental SE spectra, with the parameter values listed, together with their variances, in the first two columns of Table 1.

When all the 15 (normalized) Mueller spectra are included in the fit, we obtain the parameter values and variances shown in the last two columns of Table 1. The variances are significantly reduced (by a factor of 2) and some parameters, among which a, and R_t which are practically important quantities, are significantly smaller and certainly more accurate. Moreover, these results have been obtained after accurate determination of the actual azimuth ϕ (-1°) from the Mueller matrix elements in the off-diagonal blocks (m_{13}, m_{14}, m_{23}, m_{24}, and their transposes), which are extremely sensitive to the azimuth: for $\phi = -7°$, as initially assumed, these elements may vary by as much as 0.5. In contrast, with $\phi = -7°$ the quality of the fit of the SE spectra alone does not change, there is no clear indication of the azimuth inaccuracy, while, for instance, a is now found to be as large as 7 nm.

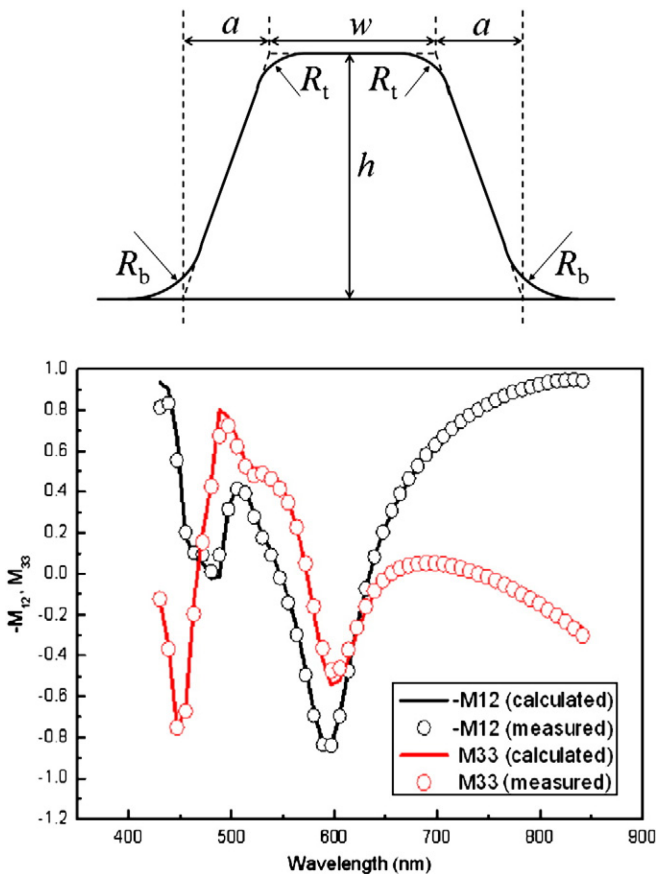

Fig. 4. Top: Trapezoidal profile with top and bottom rounded corners to used for a grating etched in bulk silicon. Bottom: typical fit of classical ellipsometric spectra taken on this grating.

Table 1
Parameter values and variances provided by the fit of the SE data (left two columns) and the fit of the full Mueller spectra (right two columns). All listed quantities are given in nm.

Parameters	Values (SE)	Variances (SE°)	Values (MP)	Variances (MP)
h	523.4	1.4	521.83	0.7
w	256.1	4.9	253.5	1.9
a	3.1	4	0.13	1.8
R_t	32.9	3.2	9.6	4.2
R_b	0	45	0	21

Angle-resolved Mueller polarimetry can also be very useful for scatterometry purposes. Typical results, taken with an isotropic sample and a resist grating on silicon are displayed on top and bottom panels of Fig. 5. The data are shown with reference polarimetric axes oriented along the radius, which materializes the local plane of the incidence for the p polarization, and perpendicular to it, for the s polarization. Moreover, due to the Abbe sine condition,

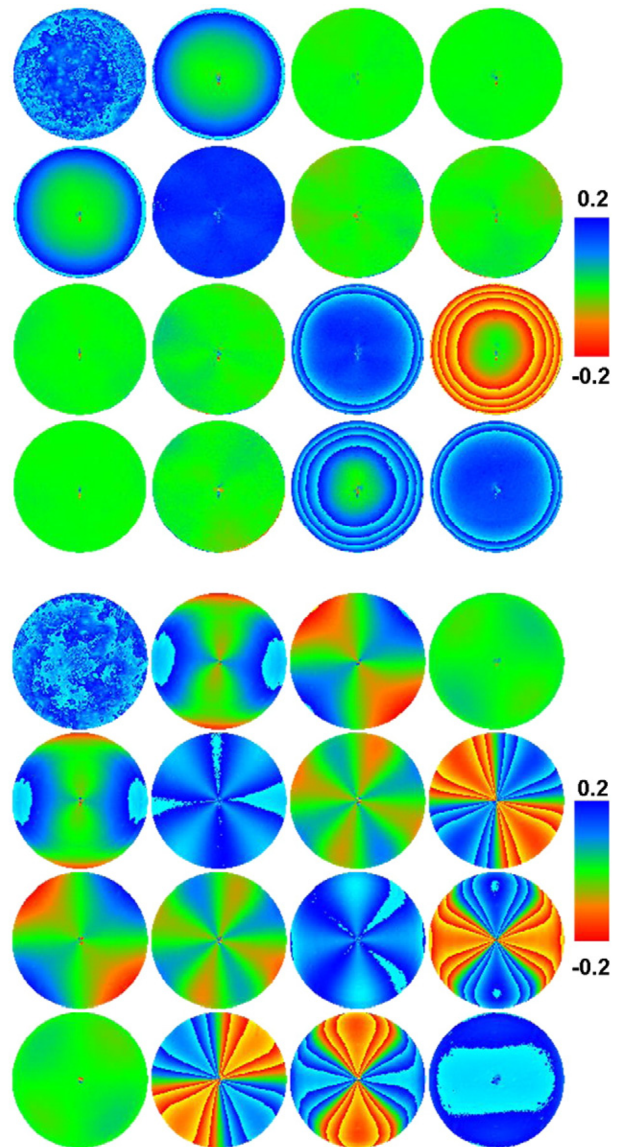

Fig. 5. Top: Angularly resolved Mueller images of a Si sample covered with a 86 nm thick layer of thermal SiO_2. The Mueller matrix elements are shown in radial (s,p) polarization coordinates. Bottom: analogous to the top panel, resist grating on Si, with nominal with a 240 nm pitch, 70 nm CD and 200 nm height. For both panels the color scale is from -0.2 (red) to 0.2 (blue) for the m_{ij} elements normalized by m_{11}.

for each point on the figure, the radial coordinate is proportional to the sine of the incidence angle, limited to 57° for these data. While for the isotropic sample the off-diagonal blocks vanish and the other elements display the expected axial symmetry, for the grating the matrix is full with a strong anisotropy. The transposition symmetries clearly show that the grating profile is symmetric. Moreover, the grating data can be accurately fitted by a trapezoidal model for the resist, with h, w and a respectively equal to 199.0, 64.4 and 0.6 nm, with variances as small as 1.1 nm for all of them. These values are in good agreement with X-SEM data taken on other, in principle identical, gratings. We point out that these very encouraging results were obtained at 633 nm operating wavelength, and should improve by shifting this wavelength to the blue. Moreover, even though these measurements were carried out with spot sizes of the order of 50 μm, due to the large numerical aperture of the objective this size may be easily reduced to a few micrometers, provided the illumination is sufficiently intense.

Similar evaluations of the polarimetric response can be carried out for many other structures, such as transistors embedded in spacers, superimposed gratings with an overlay default, 2D arrays of pillars or contact holes, and even more complex structures such as 3D photonic crystals. The interested reader will find examples of such calculations in ref. [13].

3. Discussion and conclusions

The Mueller matrix decomposition scheme based on the coherency matrix provides interesting properties through optical entropy and depolarization. This technique is a good candidate to characterize surface roughness, an essential issue for future nanotechnologies. Spectroscopic polarimetry can be addressed for in line process. Controlling the surface (spectroscopic and/or imaging) into the UV will strongly enhance the sensitivity of the technique, which may enhance or even replace the current wafer characterizations based on the bidirectional reflectance distribution function (BRDF) or the UV haze measurements.

For scatterometry purposes too, Mueller polarimetry, both in spectroscopic and in Fourier imaging modes, may offer an interesting alternative to the usual techniques based on SE measurements, due to the larger amount of data and the possibility to use the “toolboxes,” such as matrix decompositions specific for full Mueller matrices. The evaluation of the various techniques will require extensive work on well characterized samples by comparison with state of the art CD-SEM, and AFM-3D, the latter being often considered as the current “gold standard” for nanometrology.

Acknowledgement

This research was supported by the Research Fund from the French National Agency for Research (ANR-08-NANO-020-01.

References

[1] R.M.A. Azzam, N.M. Bashara, *Ellipsometry and Polarized light*, NH Elsevier, 1996, pp. 156–157.
[2] D. Ramsey, K. Ludema, Rev. Sci. Instrum. 65 (9) (1994) 2874.
[3] S.R. Cloude, SPIE (July 1999) 3754.
[4] S.R. Cloude, E. Pottier, Opt. Eng. 34 (6) (1995) 1599.
[5] J. Gil_Bernabeu, Opt. Acta 32 (1985) 259.
[6] A. Aiello, J.P. Woerdmann, Phys. Rev. Lett. (2005) 090406.
[7] M. Foldyna, C. Licitra, A. De Martino, J. Foucher, Proc. SPIE 7638 (2010) 763803.
[8] A. De Martino, S. Ben Hatit, M. Foldyna, Proc. SPIE 6518 (2007) 65180X.
[9] B. Boulbry, Thesis Université Bretagne Occidentale, 2002.
[10] M. Foldyna, A. De Martino, D. Cattelan, F. Bogeat, C. Licitra, J. Foucher, P. Barritault, J. Hazart, Proc. SPIE 7140 (2009) 71400I.
[11] “SCATMECH: Polarized Light Scattering C++ Class Library”. Th. Germer (NIST) Washington DC (USA).
[12] “Numerical Recipes in C++: The Art of Scientific Computing”. By: William H. Press (Editor), Saul A. Teukolsky (Editor), William T. Vetterling (10 Sept 2007).
[13] F. Ferrieu, 1st NanoCharM WorkshopAPI'09 (Paris, Dec.2009)and EPJ Web of Conferences 5, 2010, p. 04001.